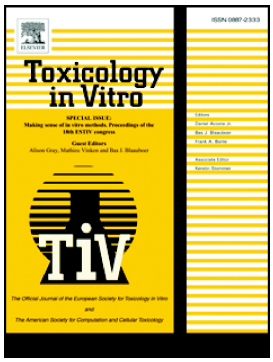

Oleocanthal and oleacein contribute to the in vitro therapeutic potential of extra virgin oil-derived extracts in non-melanoma skin cancer

Beatrice Polini, Maria Digiacomo, Sara Carpi, Simone Bertini, Francesca Gado, Giuseppe Saccomanni, Marco Macchia, Paola Nieri, Clementina Manera, Stefano Fogli

PII: S0887-2333(18)30311-4
DOI: doi:10.1016/j.tiv.2018.06.021
Reference: TIV 4316

To appear in: *Toxicology in Vitro*

Received date: 22 March 2018
Revised date: 26 June 2018
Accepted date: 27 June 2018

Please cite this article as: Beatrice Polini, Maria Digiacomo, Sara Carpi, Simone Bertini, Francesca Gado, Giuseppe Saccomanni, Marco Macchia, Paola Nieri, Clementina Manera, Stefano Fogli , Oleocanthal and oleacein contribute to the in vitro therapeutic potential of extra virgin oil-derived extracts in non-melanoma skin cancer. Tiv (2018), doi:10.1016/j.tiv.2018.06.021

Oleocanthal and oleacein contribute to the in vitro therapeutic potential of extra virgin oil-derived extracts in non-melanoma skin cancer

Beatrice Polini[a,1], Maria Digiacomo[a,b,1], Sara Carpi[a], Simone Bertini[a], Francesca Gado[a], Giuseppe Saccomanni[a], Marco Macchia[a,b], Paola Nieri[a,b], Clementina Manera[a,b,1] Stefano Fogli[c,*,1]

[a]Department of Pharmacy, University of Pisa, Pisa, Italy

[b]Interdepartmental Research Center "Nutraceuticals and Food for Health" University of Pisa, Pisa, Italy

[c]Department of Clinical and Experimental Medicine, University of Pisa, Pisa, Italy

[1]These authors contributed equally to this work

Corresponding author

Stefano Fogli

Department of Clinical and Experimental Medicine

University of Pisa

Via Roma 55

56126 Pisa

Italy

e-mail: stefano.fogli@unipi.it

Abstract

Although the anticancer properties of extra virgin olive oil (EVOO) extracts have been recognized, the role of single compounds in non-melanoma skin cancer is still unknown. The in vitro chemopreventive and anticancer action of EVOO extracts and oil-derived compounds in non-melanoma skin cancer models were evaluated on cutaneous squamous cell carcinoma cells and on immortalized human keratinocytes stimulated with epidermal growth factor. Preparation of EVOO extracts and isolation of single compounds was carried out by chromatographic methods. Antitumor activity was assessed by cell-based assays (cell viability, migration, clonogenicity, and spheroid formation) and apoptosis documented by internucleosomal DNA fragmentation. Finally, inhibition of key oncogenic signaling nodes involved in the progression from actinic keratosis to cutaneous squamous cell carcinoma was studied by western blot. EVOO extracts reduced non-melanoma skin cancer cell viability and migration, prevented colony and spheroid formation, and inhibited proliferation of atypical keratinocytes stimulated with epidermal growth factor. Such a pharmacological activity was promoted by oleocanthal and oleacein through the inhibition of Erk and Akt phosphorylation and the suppression of B-Raf expression, whereas tyrosol and hydroxytyrosol did not have effect. The current study provides in vitro evidence for new potential clinical applications of EVOO extracts and/or single oil-derived compounds in the prevention and treatment of non-melanoma skin cancers.

Key words: Oil extracts; oleocanthal; oleacein; skin cancer; anticancer activity; chemoprevention.

Abbreviations: OC: oleocanthal; OA: oleacein; T: tyrosol; HT: hydroxytyrosol.

1. Introduction

Non-melanoma skin cancer is the most common form of cancer found in the Caucasian population with increased incidence, particularly in younger age population. This type of cancer caused nearly 15,000 deaths, 3.5 million new cases, and over 3 billion dollars a year in medical expenses only in the US, representing an important problem in public health management (Rogers et al., 2010). Non-melanoma skin cancer refers to the two main types of skin cancers: basal cell carcinoma, which originates from the basal layer of the epidermis, and cutaneous squamous cell carcinoma (cSCC), which originates from the spinous layer. Although squamous cell carcinoma has a lower frequency than basal cell carcinoma, it is more aggressive with a higher probability to develop metastasis and responsible for most of deaths associated with non-melanoma skin cancer (Trakatelli et al., 2007).

Chronic solar exposure, low phototype and some genetic susceptibility factors are important etiologic factors (D'Orazio et al., 2013). Furthermore, some evidence suggests that squamous cell carcinoma may originate from actinic keratosis (AK) lesions, whose rate of progression to squamous cell carcinoma is difficult to define. The risk varies depending on lesion duration, patient's characteristics (e.g., phototype) and immunological status; overall, the rate of progression was estimated to be about 10% (Schwartz et al., 2008). The epidermal growth factor (EGF) binds to its cognate receptor EGFR leading to the activation of RAS/MEK/ERK and PI3K/Akt/mTOR pathways that play a key role in the molecular pathogenesis of both squamous cell carcinoma and actinic keratosis (Khavari, 2006; Voiculescu et al., 2016).

Polyphenols are recognized as powerful antioxidants also endowed with anti-inflammatory, antimicrobial, and antitumor properties (Pandey and Rizvi, 2009). These compounds are important constituents of many plants and vegetables. A source of

polyphenol is represented by extra virgin olive oil (EVOO). The phenolic compounds identified in EVOO can be classified into three categories: simple phenols (such as tyrosol and hydroxytyrosol), secoiridoids (such as oleuropein, oleocanthal, and oleacein), and lignans. Several lines of evidence suggest that oleocanthal has anticancer activity in different types of tumors including hepatocellular carcinoma, multiple myeloma and breast, prostate and pancreatic cancer (Akl et al., 2014; Khanfar et al., 2015; LeGendre et al., 2015). Recently, our research group demonstrated that oleocanthal exerts cytotoxic activity against human malignant melanoma cells (Fogli et al., 2016).

The current work was aimed at evaluating the in vitro anticancer and chemopreventive potential of two EVOO extracts that differ in quantitative composition of simple compounds (tyrosol and hydroxytyrosol) and secoiridoid derivatives (oleocanthal and oleacein) on cutaneous non-melanoma skin cancer models. Specifically, the A431 squamous cell carcinoma cells overexpressing EGFR (Graness et al., 2000) was selected to test the anticancer activity of extracts and compounds, as previously reported (Kang et al., 2017). The chemoprevention potential was assessed on immortalized (non-tumor) human keratinocytes (HaCaT) stimulated with EGF, a condition reproducing an in vitro microenvironment that favors the progression from actinic keratosis to cutaneous squamous cell carcinoma (Ratushny et al., 2012; Xiao et al., 2017). Finally, the activity of the secoiridoid derivatives, oleocanthal (OC) and oleacein (OA), and that of the simple phenols, tyrosol (T) and hydroxytyrosol (HT), were also investigated in the same experimental models.

2. Materials and methods

2.1 Chemistry

2.1.1 Chemical reagents and simple phenols

Solvents used for the purification procedure, HPLC analyses, and NMR analyses were purchased from Sigma-Aldrich. Evaporation was carried out under vacuum using a rotating evaporator. Silica gel flash chromatography was performed using silica gel 60Å (0.040–0.063 mm; Merck). TLC analyses were carried out on Merck aluminum silica gel (60 F254) and were visualized under a UV lamp (λ = 254 nm) or by spraying with a 10% solution of phosphomolybdic acid in absolute ethanol. Preparative TLC (Prep TLC) purification was performed using either 2 mm (20 x 10) and 1 mm (10 x 10) glass-backed sheets precoated with silica gel 60 F254 purchased from VWR. p-hydroxyphenylacetic acid (as HPLC internal standard), tyrosol, and hydroxytyrosol were purchased from Sigma-Aldrich.

2.1.2 Preparation of secoiridoid derivatives

The extraction and purification of oleocanthal and oleacein were developed using a previously reported procedure (Fogli et al., 2016). The purity of the secoiridoid derivatives was determined by 1H NMR, using a Bruker AVANCE IIITM 400 spectrometer (operating at 400 MHz) and HPLC analyses, using a Bechman HPLC instrument equipped with a system Gold UV/VIS Detector 166, setted to 278 nm. Separation was performed on a reverse phase C18 column Phenomenex using a mobile phase constituted by a mixture of H2O/AcOH (97.5:2.5 v/v) and MeOH/ACN (1:1 v/v).

2.1.3 Preparation of phytoextracts and quantification of phenolic compounds

The phytoextracts P1 and P2 were prepared starting from two different extra virgin olive oils. Briefly about 3 g of oil were mixed with n-hexane (12 ml) and acetonitrile (15 ml) and then, the mixture was homogenized using a vortex mixer. After centrifugation

at 4,000 rpm for 5 min, at 25°C, the acetonitrile phase was collected, and evaporated under reduced pressure, to afford the phytoextracts P1 and P2. The oil extract was diluted with a mixture of methanol/water (1: 1 v/v) and injected in HPLC, for analysis. Phenolic compounds were identified by comparing their retention times and UV absorbance spectra with those of the authenticated standard and quantified at 278 nm using p-hydroxyphenylacetic acid as internal standard, according to previously reported method (Tasioula-Margari and Tsabolatidou, 2015).

For each standard compound, the calibration curve was built and the detection limits (LOD) and quantification (LOQ) were estimated (Table 1). Sample concentrations were determined by linear regression. Correlation coefficients for each of the calibration curves were >0.99.

2.2 Biology

2.2.1 Cell lines

The human epidermoid carcinoma cell line A431 (ATCC, CRL-1555TM, Rockville, MD, USA) and human immortalized keratinocytes (HaCat) (ThermoFisher, Waltham, Massachusetts, USA) were cultured in DMEM (Euroclone, Euroclone, Milan, Italy) supplemented with 10% fetal bovine serum (FBS), 100 U/ml penicillin, and 100 µg/ml streptomycin (Euroclone, Milan, Italy) at 37 °C with 5% CO_2. A431-derived spheroids were cultured in DMEM/F12 (1:1) (Euroclone, Milan, Italy) supplemented with 20 ng/ml EGF (Sigma-Aldrich Milan, Italy), 0,4% BSA (Sigma-Aldrich, Milan, Italy) e 4 µg/ml insulin (Sigma-Aldrich, Milan, Italy).

2.2.2 Cell viability assay

Cell viability was measured using a method based on Neutral Red Assay (N2889, Sigma-Aldrich, Germany) following manufacturer's instructions. Briefly, cells (4×10^4/well) were seeded in 96-well plate in 10% FBS medium and after 24 h and complete medium was replaced by 1% FBS medium containing test compounds or vehicle. Phytoextracts was dissolved in DMSO (final concentration never exceeds 0.2%) and tested in a concentration range of 1-200 μg/ml for 72 h. Oleocanthal, oleacein, tyrosol and hydroxytyrosol were dissolved in DMSO (final concentration never exceeds 0.2 %) and tested at 1-100 μM for 72 h. Further experiments were performed using extracts or single compounds at concentrations that approximate the IC_{50} mean values obtained in cell viability assays, as previously reported (Kang et al., 2017).

2.2.3 Cell colony forming assay

A431 were seeded at low density (500 cells/well) in 6-well plate with 10% FBS medium and treated after 24 h with phytoextracts at concentrations that induce 50% cell growth inhibition (IC_{50}) in 1% FBS medium. After 10 days, colonies were washed twice with PBS, fixed with methanol for 20 min at -20°C, and stained with 0.05% crystal violet for 10 min at room temperature. Colonies containing >50 individual cells were counted under light microscopy. Pictures were taken at a 4× magnification.

2.2.4 Cell migration assay

Migration assay was performed using IBIDI culture inserts (IBIDI GmbH) with two different wells separated by a 500 μm wall. A431 cells (2.1×10^4 in 70 μl) were seeded into each insert and incubated at 37 °C with 5% CO_2. After 24 h, inserts were removed to create an empty space of 500 μm between the two areas of confluent cells. Dishes

were washed twice with PBS to remove detached cells and incubated with phytoextracts at their corresponding IC_{50}s. Cell migration was monitored by light microscopy (4× magnification) at different time points. The percentage decrease in the gap/darkness was calculated by using Image J software.

2.2.5 Spheroid preparation

A431 cells were seeded at low density (250 cells/well) in an optimized medium in 96-well plate coated with 1.5 % agarose to avoid cell adhesion. Cells were then treated with different concentrations of phytoextracts ranging from 1 to 200 μg/ml for 72 h and monitored by light microscopy (4× magnification) after 10 d.

2.2.7 Apoptosis

Apoptosis was evaluated for single oil-derived compounds (i.e., OC, OA, HT and T) using the Cell Death Detection ELISA Kit (Ref. 11774452001, Roche, Mannheim, Germany) as previously reported (Adinolfi et al., 2015). Briefly, Cells were treated with single compounds and lysates (obtained by 10^4 cells of each sample after 72 h) were loaded in a streptavidin-coated plate. A mixture of anti-histone-biotin and anti-DNA-POD was added into each well. After incubation for 2 h at room temperature, the number of nucleosomes in the immune-complex was quantified photometrically using the Infinite M200 NanoQuant instrument (Tecan, Salzburg, Austria) microplate reader at a wavelength of 405 nm. Specific detection of apoptosis was carried out by quantifying mono- and oligo-nucleosomes in the cytoplasmic fraction of cell lysates, whereas the supernatant was discarded.

2.2.8 Western blot

Cell lysates were collected after treatment with phytoextracts or single compounds at their corresponding IC_{50}s or vehicle for 30 min, as previously reported (Carpi et al., 2017). Samples (30 μg-protein) were separated on a 10% SDS-polyacrylamide gel electrophoresis, transferred to a nitrocellulose membrane by electro blotting (100 V, 1 h at 4°C), blocked with 5% non-fat milk in T-TBS (20 mM Tris, 500 mM NaCl, 0.1% Tween-20, pH 8) and probed with specific antibodies. Incubation was performed at 4°C overnight with anti-Erk 1/2 (Ref. sc-514302, Santa Cruz Biotechnology, Santa Cruz, CA, USA), anti-p-Erk (tyr-204) (Ref. sc-7383), anti-p-Akt1/2/3 (ser473) (Ref. Sc-7985-R, Santa Cruz Biotechnology, Santa Cruz, CA, USA) and anti-β-actin (Ref. #MAB1501, Merck Millipore, Darmstadt, Germany) antibodies. Membranes were then washed with blocking solution and probed with specific secondary antibodies. Quantification of proteins was performed using ImageJ densitometry software and signal intensities were normalized to those for β-actin.

2.2.9 Statistical analysis

All experiments were performed in triplicate and results analyzed by Prism 5 (GraphPad Software, San Diego, CA, USA). Data were shown as mean values ± standard error of the mean (SEM) obtained from at least three separate experiments. The IC_{50}s were determined using nonlinear regression curve fit. The level of statistical significance was $p<0.05$.

3. Results

3.1 Quantification of phenolic compounds

Phytoextracts (P1 and P2) were analyzed for their content in phenolic compounds (tyrosol and hydroxytyrosol) and secoiridoid derivatives (oleocanthal and oleacein). Total phenols content ranged from 400 ppm in P1 to 300 ppm in P2. For both phytoextracts, the amount of secoiridoid derivatives was higher than simple phenols. However, the ratio between secoiridoid compounds varied significantly in the two phytoextracts being 70% oleocanthal: 26% oleacein in P1, and 37% oleocanthal: 60% oleacein in P2. Simple phenols content was very low in both phytoextracts.

3.2 Activity of phytoextracts on A431 cells

P1 and P2 at 1-200 µg/ml for 72 h decreased cell viability in a concentration-dependent manner (Figure 1A) with IC_{50} values in the micromolar range (Table 2). Cell growth inhibition was maintained after replacement with phytoextracts-free medium for 72 h (Figure 1A) with similar potencies but higher maximum effect (E_{max}) than during treatment period (Table 2). Further experiments were performed using phytoextracts at concentrations that approximate their IC_{50}s calculated in cell proliferation assays (i.e., 35 and 45 µg/ml for P1 or P2, respectively).

Colony formation assay demonstrated that treatment for 10 d with phytoextracts decreased the number of colonies by approximately 60%, compared to controls (Figure 1B). Phytoextracts also time-dependently reduced cell migration. While cells were clearly out of the cell-free gap at baseline, a larger difference was seen between the two cell-covered areas in treated compared to control cells at 12 h. This represents presumably the space that the cells have not entered yet. Noteworthy, such an effect was maintained at 36 h for P1 but not P2 (Figure 1C).

Phytoextracts were tested on a three-dimensional cell culture model in which A431 cells were grown to create a spheroid structure. Spheroid formation started to occur

after 24-48 h and there was an increased compactness over time (data not shown). The 10-d analysis showed the preventive action of phytoextracts at 30 μg/ml for 72 h on spheroid formation (see the high number of satellite cells when compared to untreated plates in Figure 1D). At 50 and 100 μg/ml, satellite colonies increased, and spheroids assumed a shape with less defined and irregular edges. At the maximum concentration tested (i.e., 200 μg/ml), the loss of spheroid compactness was shown by the presence of empty spaces into the spheroid core as well as the high number of satellite cells (Figure 1D).

The mechanism of action were investigated by analyzing Erk and Akt phosphorylation and B-Raf expression in the presence or absence of phytoextracts at 35 and 45 μg/ml for P1 and P2, respectively. P1 and P2 decreased B-Raf levels by about 80 and 95%, p-Akt levels by 40 and 50%, and p-Erk expression by about 50 and 35%, respectively (Figure 2).

3.3 Activity by single oil-derived compounds on A431 cells

OC and OA at 0.1-100 μM for 72 h decreased A431 cell viability in a concentration-dependent manner (Figure 3A), with OA being the most active compound (Table 3). HT significantly reduced cell viability only at 100 μM (i.e., the maximum concentration tested), while the effect of T was negligible (Figure 3A; Table 3). Pro-apoptotic activity tested at concentrations that approximate their IC_{50} in cell viability assays (i.e., 30 μM OC and 10 μM OA) induced DNA fragmentation by 3- to 5-fold higher than controls, respectively, while HT and T did not (Figure 3B). Finally, western blot demonstrated that OC and OA had the greatest inhibitory activity on target signaling molecules, particularly on the B-Raf-Erk pathway (Figure 4).

3.4 Phytoextract activity on *HaCat cells*

HaCat cells were stimulated or not with 5 ng/ml EGF and treated with tested phytoextracts at 1-200 μg/ml for 72 h. Concentration-dependent decrease in cell viability by phytoextracts was greater in stimulated than unstimulated cells; such an effect was particularly evident for P1, whereas P2 did not reach the IC_{50} at the maximum concentration tested (Figure 5; Table 4). Noteworthy, the maximum antitumor effect by phytoextracts was strongly increased after cells were cultured in phytoextracts-free medium for further 72 h (Figure 5; Table 4).

Western blot analysis demonstrated that phytoextracts significantly reduced B-Raf expression, and Erk 1/2 and Akt phosphorylation with no significant differences between them (Figure 6).

3.5 Activity by single oil-derived compounds on EGF-stimulated HaCat cells

Single oil-derived compounds were tested at 0.1-100 μM for 72 h on EGF-stimulated cells (Figure 7A; Table 5). OC induced a concentration-dependent cell growth inhibition and was found to be more active than OA (Figure 7A; Table 5). HT also showed a concentration-dependent inhibitory effect with an IC_{50} close to the maximum tested concentration (100 μM), while T did not affect cell proliferation (Figure 7A; Table 5). Treatment with OC and OA at their IC_{50} values found in cell viability assays, induced a modest non-significant DNA fragmentation compared to untreated cells (Figure 7B). Expression levels of B-Raf, p-Akt and p-Erk proteins were decreased after treatment of stimulated cells with 25 μM OC, and 75 μM OA, T, or HT, i.e., concentrations that approximate the IC_{50} values of compounds in cell viability assays (Figure 8). In particular, OC and OA reduced B-Raf expression by approximately 70%, while HT and T

did not reach the level of significance. Accordingly, OC and OA reduced Erk and AKT phosphorylation in a greater extent than HT and T (Figure 8).

Discussion

EVOO extracts tested in the current study demonstrated to block signaling nodes that play a role in the progression from AKs to cSCCs (Ratushny et al., 2012). Such an effect was observed not only on the cutaneous squamous cell carcinoma cells but also on the immortalized (non-tumor) human keratinocytes stimulated with EGF, an in vitro model already used to identify targets for novel pharmacological strategies on AKs and cSCCs (Müller, 2009; Yadav and Denning, 2011). Such pharmacological properties of EVOO extracts may be clinically important since non-melanoma skin cancer cells typically develop on a background characterized by varying degrees of epithelial atypia and architectural disorder (Jemec et al., 2009). Specifically, cSCCs arise within AKs as a consequence of a multistage carcinogenesis process consisting in the activation of EGFR signaling cascade (with the consequent phosphorylation of Akt and Erk) and the down-regulation of p53 that eventually result in invasive cancer (Ratushny et al., 2012). Although topical application of small molecule kinase inhibitors used to treat systemic cancers has also been proposed for skin cancers (Ratushny et al., 2012), the properties of EVOO extracts found in the current study could take some advantages. For instance, concurrent multiple targeting of key signaling nodes including mTOR and B-Raf has been suggested to improve efficacy over traditional tyrosine kinase inhibitor monotherapy in melanoma patients (Etnyre et al., 2014). Furthermore, in addition to their well-recognized antioxidant effects able to promote skin protection from UVB-induced photocarcinogenesis (Budiyanto et al., 2000), we clearly demonstrated that phenolic EVOO extracts can block molecular steps that occur after the initial UV

radiation exposure and before or during tumor development (Wright et al., 2006). Our findings also shown that OC and OA were more active than T and HT, thus demonstrating that secoiridoid derivatives contribute more than simple phenols to the mechanism of action of EVOO extracts.

Molecular mechanisms other than those investigated in the current study might also account for the pharmacological activity of tested EVOO extracts. For instance, prostaglandin E2 was found to play a role in EGF-induced proliferation in HaCaT cells stimulated with EGF (Shen et al., 2004) and OC at 25 μM (i.e., a concentration that approximates the IC_{50} values obtained in the current study) has shown to inhibit the cyclooxygenase (COX) enzymes COX-1 and COX-2 by about 50% (Beauchamp et al., 2005). Furthermore, OC has been shown to be a c-met inhibitor in breast and prostate cancer cell lines with an IC_{50} range of 10-20 μM (Elnagar et al., 2011); such an effect was found to be mediated via inhibition of hepatocyte growth factor-induced c-Met activation and its downstream signaling pathways (Akl et al., 2014). Although no evidence has been provided on the role of c-met in non-melanoma skin cancer, MET expression in melanoma correlates with a lymphangiogenic phenotype.

More recently, OC was found to exert pro-apoptotic effects on human liver and colon cancer cells through ROS generation without any effect on primary normal human hepatocytes (Cusimano et al., 2017). These findings appear to be in line with those of the current study showing how OC induced internucleosomal DNA fragmentation in cSCC cells with no evidence of cytotoxicity in stimulated human keratinocyte HaCaT cells. Noteworthy, a selective pro-apoptotic activity towards cancer compared to proliferating non-cancer cells has also been shown for novel cytostatic agents used in breast cancer patients (Hu, 2015).

To our knowledge, findings of the current study demonstrated for the first time the in vitro capability of OA to induce apoptosis in cSCC cells through inhibition of key signaling pathway. Experiments in our laboratory are ongoing to further investigate the anticancer properties of oleacein in other cancer cell lines.

In the attempt to understand whether concentrations of test compounds can correspond to relevant real-life doses as human skin olive oil-derived formulations, it is worth mentioning that the OC and OA amounts in the two EVOO extracts tested were comparable to those at their IC_{50}s in single agent experiments (data not shown). T and HT levels found in EVOO extracts were instead very low and not sufficient to induce cytotoxicity.

Biofortification procedures to increase the content of phenolic compounds, i.e., oleacein and oleocanthal, in EVOO extracts (D'Amato et al., 2017) may allow obtaining topic formulations enriched with secoiridoid derivatives worthy of being tested in non-melanoma skin cancer as chemopreventive and therapeutic agents.

In conclusion, the current study provides a preclinical proof-of-concept for new potential topical applications of EVOO extracts and/or single oil-derived compounds in the prevention and treatment of non-melanoma skin cancers.

Conflicts of interest statement

The authors declare no conflict of interest.

Tables

Table 1. Chromatographic method.

Mobil phase	Fractions	Volume (ml)
100 % $CHCl_3$	1	500
95:5% $CHCl_3$/AcOEt	2-14	200
90:10% $CHCl_3$/AcOEt	15-27	200
85:15% $CHCl_3$/AcOEt	28-40	200
80:20% $CHCl_3$/AcOEt	41-53	200
75:25% $CHCl_3$/AcOEt	54-66	200
70:30% $CHCl_3$/AcOEt	67-79	200
65:35% $CHCl_3$/AcOEt	80-92	200
60:40% $CHCl_3$/AcOEt	93-105	200
55:45% $CHCl_3$/AcOEt	106-108	200
50:50% $CHCl_3$/AcOEt	109-145	600
0:100% AcOEt	146-170	400

Table 2. Potency and maximum effect of phytoextracts after treatment of A431 cells for 72 h and followed by a growth with fresh phytoextracts-free medium (72+72 h).

	IC_{50} (µg/ml ± SD)		E_{max} (% of cells ± SD)*	
	72 h	72+72 h	*72 h*	*72+72 h*
P1	37.4 ± 1.1	42.4 ± 1	29.8 ± 3.8	3.2 ± 3.1
P2	46 ± 1.1	53.7 ± 1	41.1 ± 4.1	0.45 ± 2.5

IC_{50}: concentrations that induce 50% cell growth inhibition; E_{max}: maximum effect.
*E_{max} values are expressed as a percentage of remaining tumor cells (the lower the value, the higher the maximum effect).

Table 3. Potency and maximum effect of single compounds after treatment of A431 cells for 72 h.

Compound	IC_{50} (μM ± SD)	E_{max} (% of cells ± SD)*
OC	30 ± 1.1	10.5 ± 3.6
OA	10 ± 1.1	6.8 ± 3.1
HT	>50	39 ± 90§
T	>100	NR

IC_{50}: concentrations that induce 50% cell growth inhibition; E_{max}: maximum effect. *E_{max} values are expressed as a percentage of remaining tumor cells (the lower the value, the higher the maximum effect). §Mean value obtained at the maximum concentration (i.e., 100 μM). NR: not reached.

Table 4. Potency and maximum effect of phytoextracts after treatment of EGF-stimulated Hacat cells for 72 h and followed by a growth with fresh phytoextracts-free medium (72+72 h).

	IC_{50} (µg/ml ± SD)		E_{max} (% of cells ± SD)*	
	72 h	*144 h*	*72 h*	*144 h*
P1	61 ± 1.2	53.9 ± 1	20.2 ± 11.1	1 ± 2.6
P2	>200	43.1 ± 1	62.5 ± 29.9§	3.6 ± 2.9

IC_{50}: concentrations that induce 50% cell growth inhibition; E_{max}: maximum effect. *E_{max} values are expressed as a percentage of remaining tumor cells (the lower the value, the higher the maximum effect). §Mean value obtained at the maximum concentration (i.e., 200 µg/ml).

Table 5. Potency and maximum effect of single compounds after treatment of EGF-stimulated Hacat cells for 72 h.

Compound	IC_{50} (μM ± SD)	E_{max} (% of cells ± SD)*
OC	26 ± 1.1	18.3 ± 7.2
OA	76 ± 3	33.4 ± 1.4§
HT	≈100	NR
T	>100	NR

IC_{50}: concentrations that induce 50% cell growth inhibition; E_{max}: maximum effect. *E_{max} values are expressed as a percentage of remaining tumor cells (the lower the value, the higher the maximum effect). §Mean value obtained at the maximum concentration (i.e., 100 μM). NR: not reached.

Figure legends

Figure 1

Pharmacological activity of phytoextracts on A431 cells. (A) Cell viability A431 cells treated with phytoextracts (P1 and P2) at 1-200 μg/ml for 72 h or maintained for further 72 h in phytoextracts-free medium. (B) Colony formation assay after 10 d in cells treated with P1 and P2 at 35 and 45 μg/ml, respectively, as compared to controls, (C) Scratch assay after 12 and 36 h in cells treated with phytoextracts at concentrations as colony formation assay, compared to controls. (D) Images of spheroid formation in treated (30-200 μg/ml) and control cells after 10 d and relative spheroid core densititometry. Data presented as mean ± SD of at least three independent experiments. *p<0.05, **p<0.01, ***p<0.001, as compared to control (Student's t-test or one-way ANOVA followed by Dunnetts's test for multiple comparison).

Figure 2

Western blot analysis of B-Raf, p-Erk, and p-Akt in A431 cells treated with phytoextracts. Cells were treated with phytoextract 1 (P1) and phytoextract 2 (P2) at 35 and 45 μg/ml, respectively, for 30 min. β-actin was used as a loading control. Data presented as mean ± SD of at least three independent experiments. *p<0.05, **p<0.01, ***p<0.001, as compared to control (one-way ANOVA followed by Dunnetts's multiple comparison test).

Figure 3

Apoptosis by single oil-derived compounds on A431 cells. Cells were treated with 30 μM oleocanthal (OC), 10 μM oleacein (OA), 100 μM hydroxytyrosol (HT) and tyrosol (T), for

72 h. Data presented as mean ± SD of at least three independent experiments. ***p<0.001, as compared to control (one-way ANOVA followed by Dunnetts's multiple comparison test).

Figure 4

Western blot analysis of B-Raf, p-Erk, and p-Akt in A431 cells treated with single oil-derived compounds. Cells were treated with 30 μM OC, 10 μM OA, and 100 μM HT or T for 30 min. β-actin was used as a loading control. Data presented as mean ± SD of at least three independent experiments. *p<0.05, **p<0.01, as compared to control (one-way ANOVA followed by Dunnetts's multiple comparison test).

Figure 5

Pharmacological activity of phytoextracts in HaCaT cells stimulated or not with 5 ng/ml EGF. Cell viability in stimulated and unstimulated cells treated with phytoextracts (P1 and P2) at 1-200 μg/ml for 72 h and in stimulated cells maintained for further 72 h in phytoextracts-free medium. Data presented as mean ± SD of at least three independent experiments.

Figure 6

Western blot analysis of B-Raf, p-Erk, and p-Akt in EGF-stimulated HaCaT cells treated with phytoextracts. Cells were treated with P1 or P2 at 35 and 45 μg/ml, respectively, for 30 min. β-actin was used as a loading control. Data presented as mean ± SD of at least three independent experiments. *p<0.05, **p<0.01, as compared to control (one-way ANOVA followed by Dunnetts's multiple comparison test).

Figure 7

Apoptosis by single oil-derived compounds on HaCaT cells. Cells were treated with 25 μM oleocanthal (OC), 100 μM oleacein (OA), hydroxytyrosol (HT) and tyrosol (T), for 72 h. Data presented as mean ± SD of at least three independent experiments.

Figure 8

Western blot analysis of B-Raf, p-Erk, and p-Akt in EGF-stimulated HaCaT cells treated with single-oil derived compounds. Cells were treated with 25 μM oleocanthal (OC), 100 μM oleacein (OA), hydroxytyrosol (HT) and tyrosol (T), for 30 min. β-actin was used as a loading control. Data presented as mean ± SD of at least three independent experiments. *$p<0.05$, **$p<0.01$, as compared to control (one-way ANOVA followed by Dunnetts's multiple comparison test).

References

Adinolfi, B., Carpi, S., Romanini, A., Da Pozzo, E., Castagna, M., Costa, B., Martini, C., Olesen, S.-P., Schmitt, N., Breschi, M.C., Nieri, P., Fogli, S., 2015. Analysis of the Antitumor Activity of Clotrimazole on A375 Human Melanoma Cells. Anticancer Research 35, 3781–3786.

Akl, M.R., Ayoub, N.M., Mohyeldin, M.M., Busnena, B.A., Foudah, A.I., Liu, Y.-Y., Sayed, K.A.E., 2014. Olive phenolics as c-Met inhibitors: (-)-Oleocanthal attenuates cell proliferation, invasiveness, and tumor growth in breast cancer models. PLoS ONE 9, e97622. doi:10.1371/journal.pone.0097622

Beauchamp, G.K., Keast, R.S.J., Morel, D., Lin, J., Pika, J., Han, Q., Lee, C.-H., Smith, A.B., Breslin, P.A.S., 2005. Phytochemistry: ibuprofen-like activity in extra-virgin olive oil. Nature 437, 45–46. doi:10.1038/437045a

Budiyanto, A., Ahmed, N.U., Wu, A., Bito, T., Nikaido, O., Osawa, T., Ueda, M., Ichihashi, M., 2000. Protective effect of topically applied olive oil against photocarcinogenesis following UVB exposure of mice. Carcinogenesis 21, 2085–2090.

Cusimano, A., Balasus, D., Azzolina, A., Augello, G., Emma, M.R., Di Sano, C., Gramignoli, R., Strom, S.C., McCubrey, J.A., Montalto, G., Cervello, M., 2017. Oleocanthal exerts antitumor effects on human liver and colon cancer cells through ROS generation. Int. J. Oncol. 51, 533–544. doi:10.3892/ijo.2017.4049

D'Amato, R., Proietti, P., Onofri, A., Regni, L., Esposto, S., Servili, M., Businelli, D., Selvaggini, R., 2017. Biofortification (Se): Does it increase the content of phenolic compounds in virgin olive oil (VOO)? PLoS ONE 12, e0176580. doi:10.1371/journal.pone.0176580

D'Orazio, J., Jarrett, S., Amaro-Ortiz, A., Scott, T., 2013. UV radiation and the skin. Int J Mol Sci 14, 12222–12248. doi:10.3390/ijms140612222

Elnagar, A.Y., Sylvester, P.W., Sayed, El, K.A., 2011. (-)-Oleocanthal as a c-Met inhibitor for the control of metastatic breast and prostate cancers. Planta Med. 77, 1013–1019. doi:10.1055/s-0030-1270724

Etnyre, D., Stone, A.L., Fong, J.T., Jacobs, R.J., Uppada, S.B., Botting, G.M., Rajanna, S., Moravec, D.N., Shambannagari, M.R., Crees, Z., Girard, J., Bertram, C., Puri, N., 2014. Targeting c-Met in melanoma: mechanism of resistance and efficacy of novel combinatorial inhibitor therapy. Cancer Biol. Ther. 15, 1129–1141. doi:10.4161/cbt.29451

Fogli, S., Arena, C., Carpi, S., Polini, B., Bertini, S., Digiacomo, M., Gado, F., Saba, A., Saccomanni, G., Breschi, M.C., Nieri, P., Manera, C., Macchia, M., 2016. Cytotoxic Activity of Oleocanthal Isolated from Virgin Olive Oil on Human Melanoma Cells. Nutr Cancer 68, 873–877. doi:10.1080/01635581.2016.1180407

Graness, A., Hanke, S., Boehmer, F.D., Presek, P., Liebmann, C., 2000. Protein-tyrosine-phosphatase-mediated epidermal growth factor (EGF) receptor transinactivation and EGF receptor-independent stimulation of mitogen-activated protein kinase by bradykinin in A431 cells. Biochem. J. 347, 441–447.

Hu, W., 2015. Abstract 1635: Mechanistic investigation of neutropenia associated with palbociclib. Cancer Res. 75, 1635–1635. doi:10.1158/1538-7445.AM2015-1635

Jemec, G., Kemeny, L., Miech, D., 2009. Non-Surgical Treatment of Keratinocyte Skin Cancer. Springer Science & Business Media.

Kang, T.-H., Yoon, G., Kang, I.-A., Oh, H.-N., Chae, J.-I., Shim, J.-H., 2017. Natural Compound Licochalcone B Induced Extrinsic and Intrinsic Apoptosis in Human Skin

Melanoma (A375) and Squamous Cell Carcinoma (A431) Cells. Phytother Res 31, 1858–1867. doi:10.1002/ptr.5928

Khanfar, M.A., Bardaweel, S.K., Akl, M.R., Sayed, El, K.A., 2015. Olive Oil-derived Oleocanthal as Potent Inhibitor of Mammalian Target of Rapamycin: Biological Evaluation and Molecular Modeling Studies. Phytother Res 29, 1776–1782. doi:10.1002/ptr.5434

Khavari, P.A., 2006. Modelling cancer in human skin tissue. Nat. Rev. Cancer 6, 270–280. doi:10.1038/nrc1838

LeGendre, O., Breslin, P.A.S., Foster, D.A., 2015. (-)-Oleocanthal rapidly and selectively induces cancer cell death via lysosomal membrane permeabilization (LMP). Molecular & Cellular Oncology 00–00. doi:10.1080/23723556.2015.1006077

Müller, B.A., 2009. Imatinib and its successors--how modern chemistry has changed drug development. Current Pharmaceutical Design 15, 120–133.

Pandey, K.B., Rizvi, S.I., 2009. Plant polyphenols as dietary antioxidants in human health and disease. Oxid Med Cell Longev 2, 270–278. doi:10.4161/oxim.2.5.9498

Ratushny, V., Gober, M.D., Hick, R., Ridky, T.W., Seykora, J.T., 2012. From keratinocyte to cancer: the pathogenesis and modeling of cutaneous squamous cell carcinoma. J. Clin. Invest. 122, 464–472. doi:10.1172/JCI57415

Rogers, H.W., Weinstock, M.A., Harris, A.R., Hinckley, M.R., Feldman, S.R., Fleischer, A.B., Coldiron, B.M., 2010. Incidence estimate of nonmelanoma skin cancer in the United States, 2006. Arch Dermatol 146, 283–287. doi:10.1001/archdermatol.2010.19

Schwartz, R.A., Bridges, T.M., Butani, A.K., Ehrlich, A., 2008. Actinic keratosis: an occupational and environmental disorder. J Eur Acad Dermatol Venereol 22, 606–615. doi:10.1111/j.1468-3083.2008.02579.x

Shen, S.-C., Ko, C.-H., Hsu, K.-C., Chen, Y.-C., 2004. 3-OH flavone inhibition of epidermal growth factor-induced proliferaton through blocking prostaglandin E2 production. Int. J. Cancer 108, 502–510. doi:10.1002/ijc.11581

Tasioula-Margari, M., Tsabolatidou, E., 2015. Extraction, Separation, and Identification of Phenolic Compounds in Virgin Olive Oil by HPLC-DAD and HPLC-MS. Antioxidants (Basel) 4, 548–562. doi:10.3390/antiox4030548

Trakatelli, M., Ulrich, C., del Marmol, V., Euvrard, S., Euvard, S., Stockfleth, E., Abeni, D., 2007. Epidemiology of nonmelanoma skin cancer (NMSC) in Europe: accurate and comparable data are needed for effective public health monitoring and interventions. Br. J. Dermatol. 156 Suppl 3, 1–7. doi:10.1111/j.1365-2133.2007.07861.x

Voiculescu, V., Calenic, B., Ghita, M., Lupu, M., Caruntu, A., Moraru, L., Voiculescu, S., Ion, A., Greabu, M., Ishkitiev, N., Caruntu, C., 2016. From Normal Skin to Squamous Cell Carcinoma: A Quest for Novel Biomarkers. Dis. Markers 2016, 4517492–14. doi:10.1155/2016/4517492

Wright, T.I., Spencer, J.M., Flowers, F.P., 2006. Chemoprevention of nonmelanoma skin cancer. J. Am. Acad. Dermatol. 54, 933–46– quiz 947–50. doi:10.1016/j.jaad.2005.08.062

Xiao, T., Zhu, J.J., Huang, S., Peng, C., He, S., Du, J., Hong, R., Chen, X., Bode, A.M., Jiang, W., Dong, Z., Zheng, D., 2017. Phosphorylation of NFAT3 by CDK3 induces cell transformation and promotes tumor growth in skin cancer. Oncogene 36, 2835–2845. doi:10.1038/onc.2016.434

Yadav, V., Denning, M.F., 2011. Fyn is induced by Ras/PI3K/Akt signaling and is required for enhanced invasion/migration. Mol. Carcinog. 50, 346–352. doi:10.1002/mc.20716

Highlights

- Extra virgin olive oil (EVOO) extracts exert anticancer activity on squamous cell carcinoma
- EVOO extracts prevent proliferation of atypical human keratinocytes stimulated with EGF
- EVOO extracts reduce protein expression of B-Raf and phosphorylation of Erk 1/2 and Akt
- Oleocanthal and oleacein contribute to the anticancer effects by phytoextracts

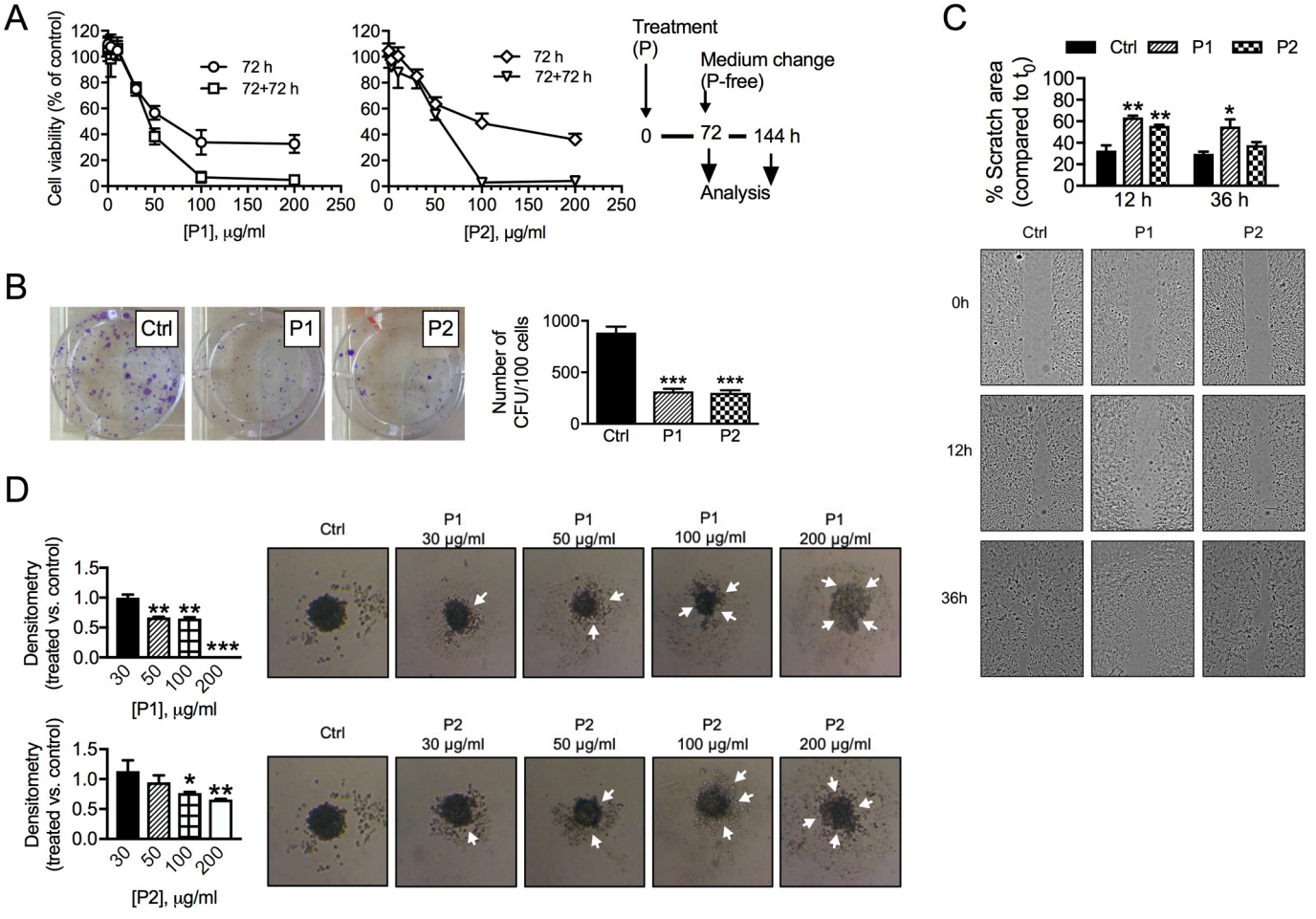
A
Cell viability (% of control)
72 h
72+72 h
[P1], μg/ml
[P2], μg/ml
Treatment
(P)
Medium change
(P-free)
0
72
144 h
Analysis
B
Ctrl
P1
P2
Number of CFU/100 cells
C
% Scratch area (compared to t0)
12 h
36 h
0h
12h
36h
D
Densitometry (treated vs. control)
[P1], μg/ml
[P2], μg/ml
30 μg/ml
50 μg/ml
100 μg/ml
200 μg/ml

Figure 1

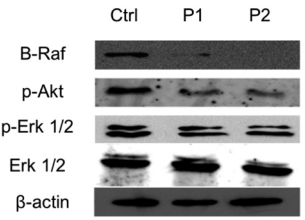
Ctrl
P1
P2
B-Raf
p-Akt
p-Erk 1/2
Erk 1/2
β-actin

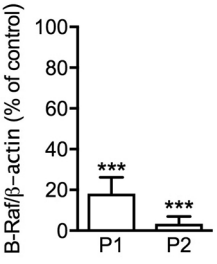
B-Raf/β-actin (% of control)
100
80
60
40
20
0
***
***
P1
P2

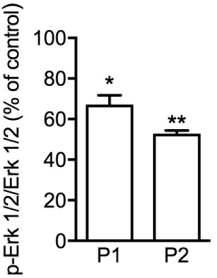
p-Erk 1/2/Erk 1/2 (% of control)
100
80
60
40
20
0
*
**
P1
P2

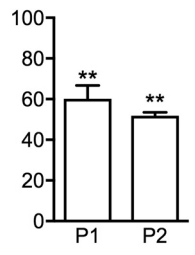
p-Akt/β-actin (% of control)
100
80
60
40
20
0
**
**
P1
P2

Figure 2

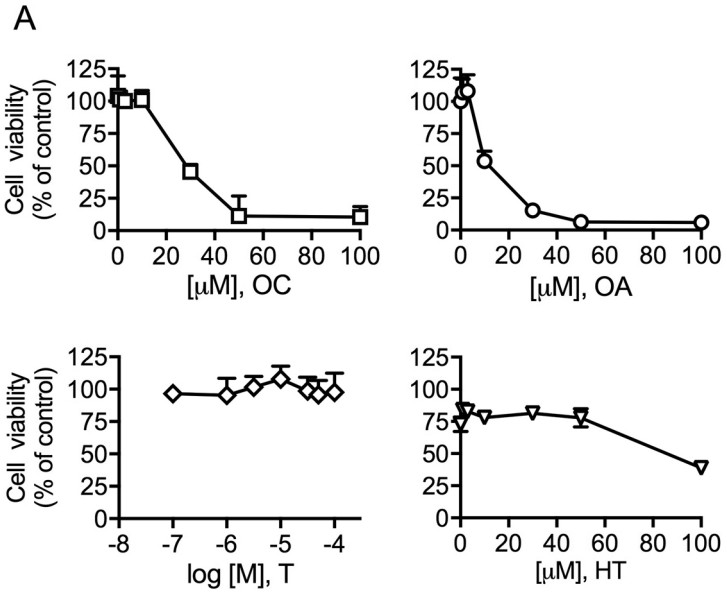
A
Cell viability (% of control)
125
100
75
50
25
0
0 20 40 60 80 100
[μM], OC
[μM], OA
-8 -7 -6 -5 -4
log [M], T
[μM], HT

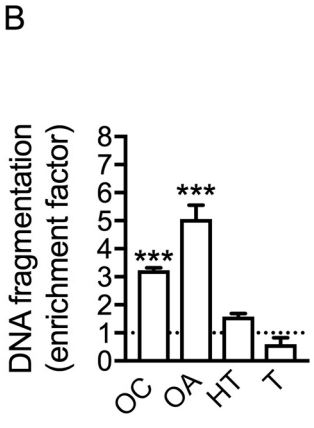
B
DNA fragmentation (enrichment factor)
8
7
6
5
4
3
2
1
0
***
***
OC
OA
HT
T

Figure 3

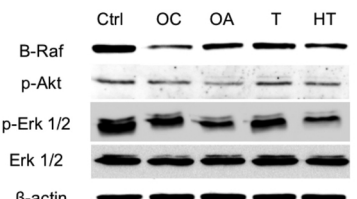
Ctrl
OC
OA
T
HT
B-Raf
p-Akt
p-Erk 1/2
Erk 1/2
β-actin

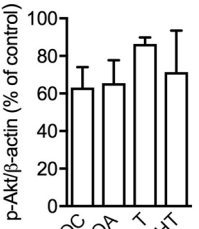
p-Akt/β-actin (% of control)
100
80
60
40
20
0
OC
OA
T
HT

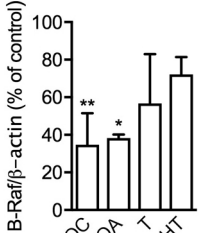
B-Raf/β-actin (% of control)
100
80
60
40
20
0
**
*
OC
OA
T
HT

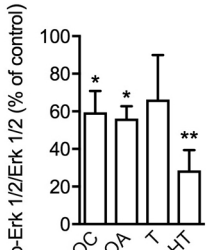
p-Erk 1/2/Erk 1/2 (% of control)
100
80
60
40
20
0
*
*
**
OC
OA
T
HT

Figure 4

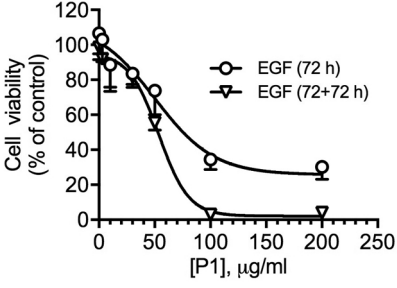
Cell viability
(% of control)
EGF (72 h)
EGF (72+72 h)
[P1], μg/ml

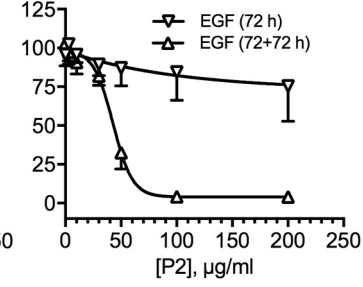
EGF (72 h)
EGF (72+72 h)
[P2], μg/ml

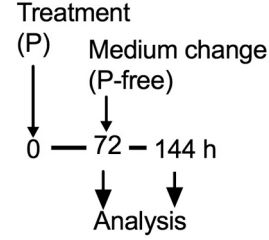
Treatment
(P)
Medium change
(P-free)
0
72
144 h
Analysis

Figure 5

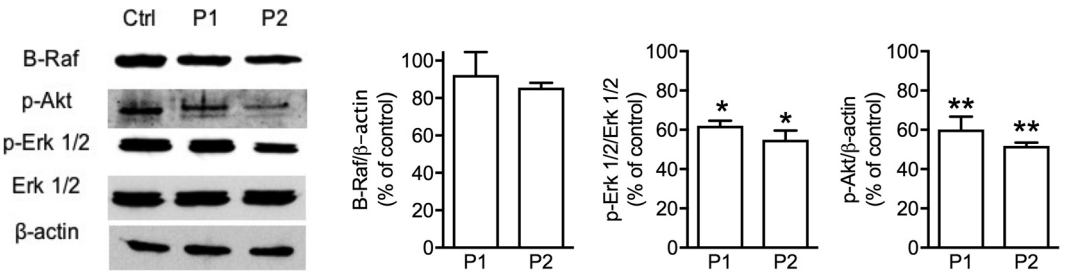
Ctrl
P1
P2
B-Raf
p-Akt
p-Erk 1/2
Erk 1/2
β-actin
B-Raf/β−actin (% of control)
p-Erk 1/2/Erk 1/2 (% of control)
p-Akt/β-actin (% of control)
100
80
60
40
20
0
*
**
P1
P2

Figure 6

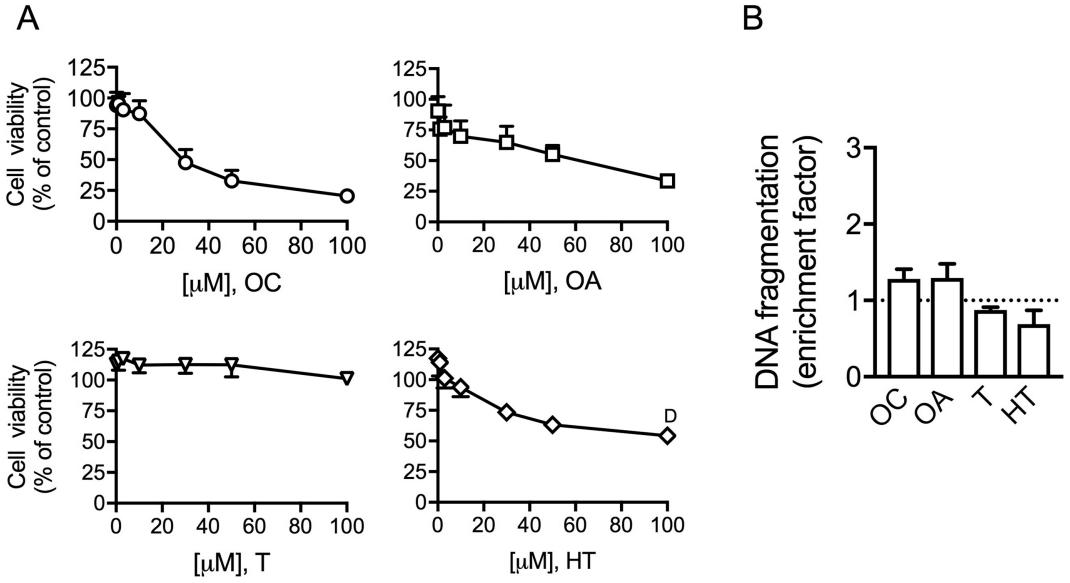
A
B
Cell viability (% of control)
125
100
75
50
25
0
0 20 40 60 80 100
[μM], OC
[μM], OA
[μM], T
[μM], HT
D
DNA fragmentation (enrichment factor)
3
2
1
0
OC
OA
T
HT

Figure 7

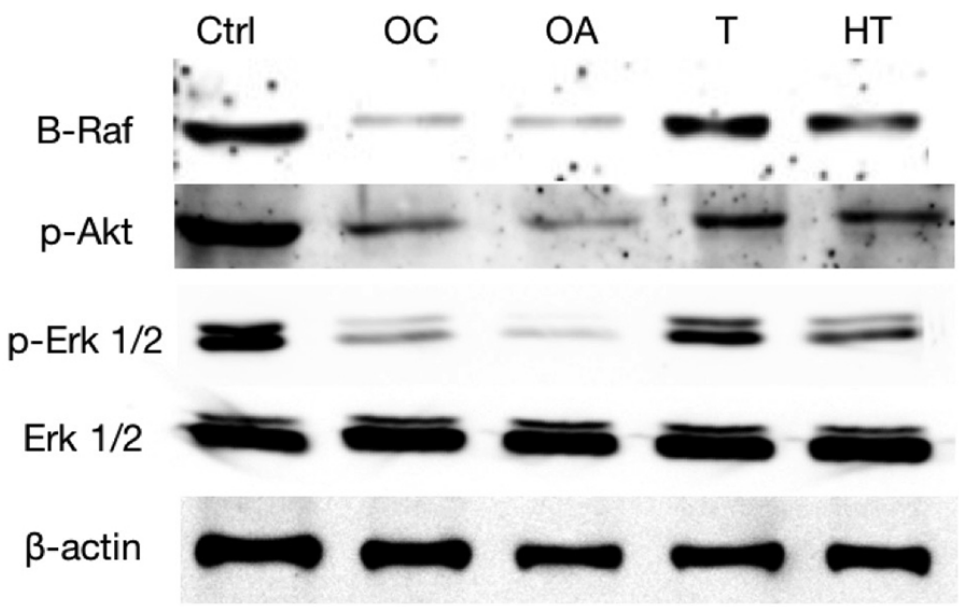
Ctrl
OC
OA
T
HT
B-Raf
p-Akt
p-Erk 1/2
Erk 1/2
β-actin

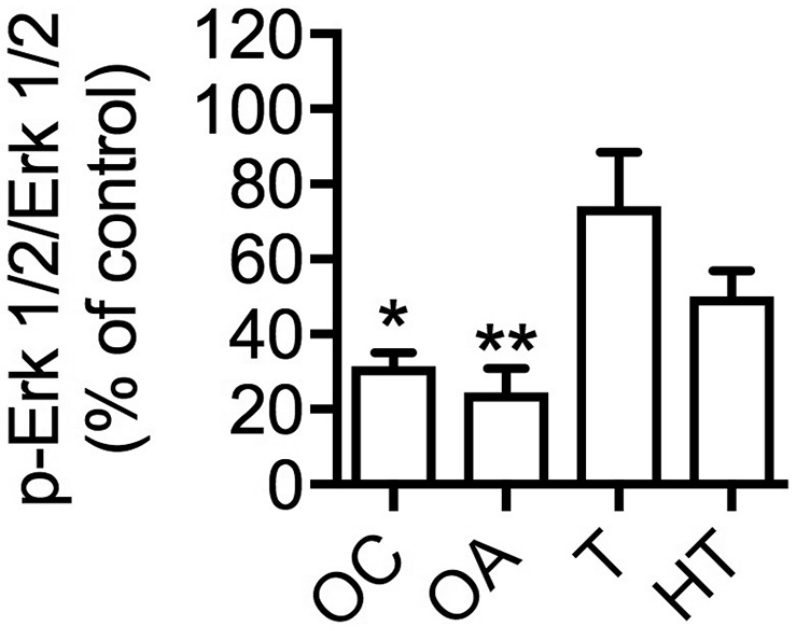
p-Erk 1/2/Erk 1/2
(% of control)
120
100
80
60
40
20
0
*
**
OC
OA
T
HT

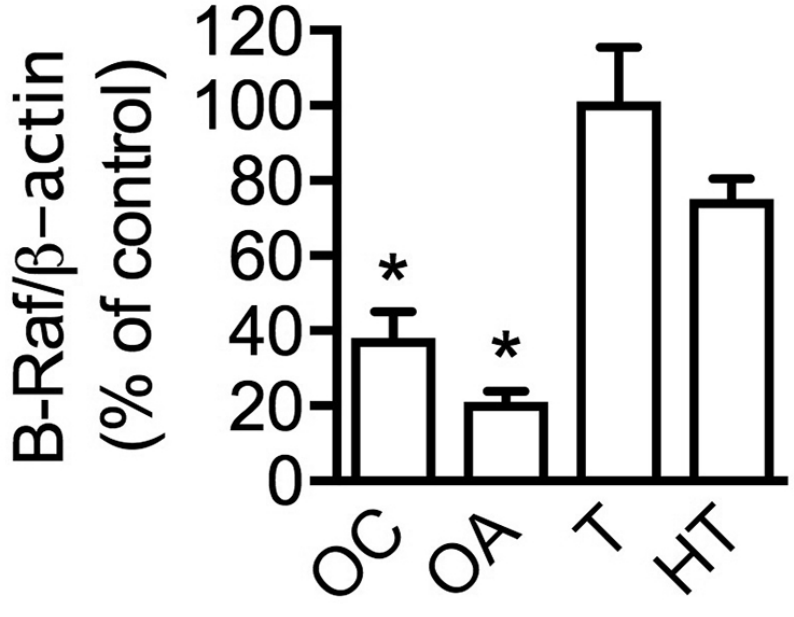
B-Raf/β−actin
(% of control)
120
100
80
60
40
20
0
*
*
OC
OA
T
HT

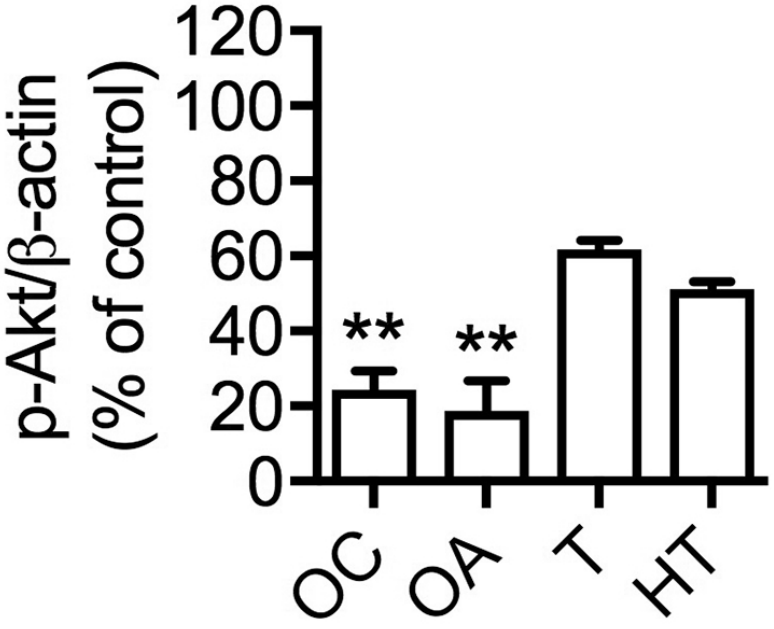
p-Akt/β-actin
(% of control)
120
100
80
60
40
20
0
**
**
OC
OA
T
HT

Figure 8